J Soils Sediments (2012) 12:1517–1529
DOI 10.1007/s11368-012-0588-8

IASWS 2011: THE INTERACTIONS BETWEEN SEDIMENTS AND WATER

Microphytobenthic production estimated by in situ oxygen microprofiling: short-term dynamics and carbon budget implications

Lionel Denis · François Gevaert · Nicolas Spilmont

Received: 8 July 2011 / Accepted: 12 August 2012 / Published online: 14 September 2012

Abstract
Purpose Short-term temporal variability of microphytobenthic primary production is suspected to be of the same magnitude as seasonal variability, but data remain very scarce due to methodological limitations. In this context, a 6-day in situ high-frequency survey was performed in a temperate intertidal mudflat using an automated microprofiling system.
Materials and methods In situ microphytobenthic primary production was measured using an automated acquisition system for oxygen microprofiles. More than 900 microprofiles, acquired during six consecutive days in April 2008, allowed the establishment of robust relationships between oxygen production and irradiance. Moreover, simultaneous measurements of fluorescence parameters and oxygen microprofiles during two diurnal emersion periods led to significant correlations between relative electron transport rate (rETR) and gross oxygen production (GOP).
Results and discussion The use of an automated system allowed the estimation of oxygen exchanges during both immersion and emersion periods, and to our knowledge, this is the first study presenting continuous measurements during six consecutive days. The intertidal mudflat studied here was characterized by a maximum net oxygen production of 6.74 $mmol O_2 m^{-2} h^{-1}$. Evidence for microphytobenthic migration behavior was observed during several periods and induced important depletion in oxygen production while irradiance remained high. Consequently, estimations of GOP from fitted photosynthesis–irradiance curves (*P–I* curves) showed an overestimation of 31 % compared to the GOP actually measured during the whole deployment.
Conclusions This study confirmed that oxygen microsensors may be used to record microphytobenthic primary production, as resulting dynamics agreed with fluorescence data, while production values were in accordance with those presented in the literature. High-frequency microprofiles acquisition may be an easy way to monitor short-term temporal changes in microphytobenthic primary production in order to calculate accurate carbon or oxygen budgets for intertidal areas.

Keywords Intertidal mudflat · Microphytobenthos · Migratory behavior · Modulated fluorescence · Oxygen microprofiling · Temporal variability

Responsible editor: Geraldene Wharton

L. Denis (✉) · F. Gevaert · N. Spilmont
Université Lille Nord de France,
1 bis Rue Georges Lefevre,
59000 Lille, France
e-mail: Lionel.denis@univ-lille1.fr

L. Denis · F. Gevaert · N. Spilmont
Université des Sciences et Technologies de Lille,
Station Marine de Wimereux,
62930 Wimereux, France

L. Denis · F. Gevaert · N. Spilmont
UMR 8187 LOG, CNRS,
28, Avenue Foch,
62930 Wimereux, France

L. Denis
Departamento de Hidrobiología–UMR 7294 MIO,
IRD México–Universidad Autónoma Metropolitana,
Av. San Rafael Atlixco n°186, Col. Vicentina,
09340 Iztapalapa México DF, México

1 Introduction

Intertidal areas—located between terrestrial and marine domains—are subject to high discharges of nutrients and organic matter from freshwaters. A large fraction of coastal organic carbon production and mineralization occurs in these areas, particularly in mudflats where the accumulation of organic matter and nutrients in surficial sediments leads

to high mineralization rates and conditions support active primary production. In macrotidal temperate estuaries, phytoplankton primary production is generally limited by high turbidity levels in the water column due to suspended sediment (Cloern 1987), and a large part of estuarine primary production may be attributed to microphytobenthic organisms living at the surface of the sediment (Guarini et al. 1998; Montani et al. 2003) and submitted to daily air exposure.

As a consequence of day–night and low–high tide cycles, microphytobenthic organisms are also subject to large short-term variations of physical and chemical parameters (e.g., hydrodynamic regime, light and nutrient availability, temperature, salinity), which influence the spatial and temporal distribution of their biomass as well as their photosynthetic activity. In these unstable ecosystems, numerous microphytobenthic taxa exhibit a migration behavior which is known to widely affect the temporal and spatial distribution and production by microphytobenthos (Consalvey et al. 2004; Easley et al. 2005). Light and tidal rhythms are generally considered as the main factors influencing migration processes (Serôdio et al. 1997), but several other parameters may interfere with algae migration behavior, such as nutrients or CO_2 limitation, rain, or predators (see Consalvey et al. (2004) for a review).

In the last couple of decades, studies of intertidal microphytobenthic primary production were made easier with the development of non-destructive in situ methods (oxygen microsensors: Revsbech and Jorgensen (1983), Pinckney and Zingmark (1991); pulse amplitude modulation (PAM) fluorometry: Barranguet and Kromkamp (2000), Serôdio et al. (2005); spectral reflectance analysis (SRA): Paterson et al. (1998), Carrère et al. (2004)) that minimize perturbations of natural gradients and environmental conditions. However, accurate estimations remain scarce, notably due to short-term variability in the photosynthetic activity of microphytobenthos. This short-term variability is recognized to have a similar magnitude to the seasonal variation (Blanchard et al. 2006), and it has been suggested by Macintyre and Cullen (1996) that daily measurement should be carried out in order to produce more accurate estimations of global primary production. Although a few studies deal with short-term variability of primary production (Serôdio et al. 2005), most estimations are based on seasonal, monthly, or weekly measurements and do not take into account variations at shorter time scales (daily or hourly variations).

Since the pioneering work of Revsbech et al. (1981) and Revsbech and Jorgensen (1983), the oxygen microprofiling technique has been used extensively to understand microphytobenthos behavior and quantify its photosynthetic rate (e.g., Glud et al. 1992; Pinckney and Zingmark 1993; Epping and Jorgensen 1996; Glud et al. 2002; Gerbersdorf et al. 2004; Serôdio et al. 2007). Nowadays, this approach is particularly useful because profile acquisition can be automated and rapidly done in situ, and data may be checked in real time for intertidal or shallow subtidal areas (Denis and Desreumaux 2009). Profile measurements can be performed with limited perturbations of adjacent sediments or modification of the environment, in contrast with methods using enclosures where the effects of the imposed hydrodynamics must be evaluated, especially in shallow coastal areas (Jørgensen and Boudreau 2001). Moreover, oxygen microprofiles give valuable information on the vertical distribution of production rates, while the approach using enclosures generally consider the sediment as a "black box". Finally, "surficial" methods such as PAM fluorometry or SRA remain controversial because algal fluorescence from below the sediment–water interface can contribute significantly to the fluorescence measured at the sediment surface, causing overestimates of the true apparent quantum efficiency at higher irradiances (Kromkamp and Forster 2006). Unfortunately, due to the very small surface area investigated with microsensor measurements, accurately taking into account the spatial heterogeneity remains a challenge, while infaunal activity and microphytobenthic photosynthesis contribute to the presence of micro-niches and "hot spots" of intense production and consumption (Glud et al. 1996, 1999; Wenzhöfer and Glud 2004). Moreover, during the immersion period, the use of microsensors may also modify the diffusive boundary layer, hence leading to overestimation of sediment–water fluxes (Glud et al. 1994). Despite these limitations, the use of microsensors allows for the continuous application of the same method—during emersion, immersion, and transition periods—which is of prime importance for short-term studies, such as the one presented here.

In this context, this paper presents the results of in situ measurements using an automated oxygen microprofiling system. Continuous measurements of oxygen concentrations were performed during six consecutive days in an intertidal mudflat, in order to monitor the dynamics of microphytobenthic activity. Furthermore, concurrent measurements were performed with a PAM fluorometer to assess whether oxygen production rates were consistent with PAM-derived measurements of photosynthetic activity. Indeed, variable fluorescence techniques have been used for about 10 years to study photosynthetic processes in marine ecology (Perkins et al. 2002), and PAM fluorometer results have been successfully correlated with other methods such as benthic incubation chambers (Migné et al. 2007) or ^{14}C incubations (Barranguet and Kromkamp 2000). We further discuss the capabilities of the microprofiling system as a tool to monitor microphytobenthic migration.

2 Materials and methods

2.1 Study site

Measurements and sampling were carried out on an intertidal mudflat located in the Canche estuary (Fig. 1) situated in the eastern English Channel. This macrotidal estuary

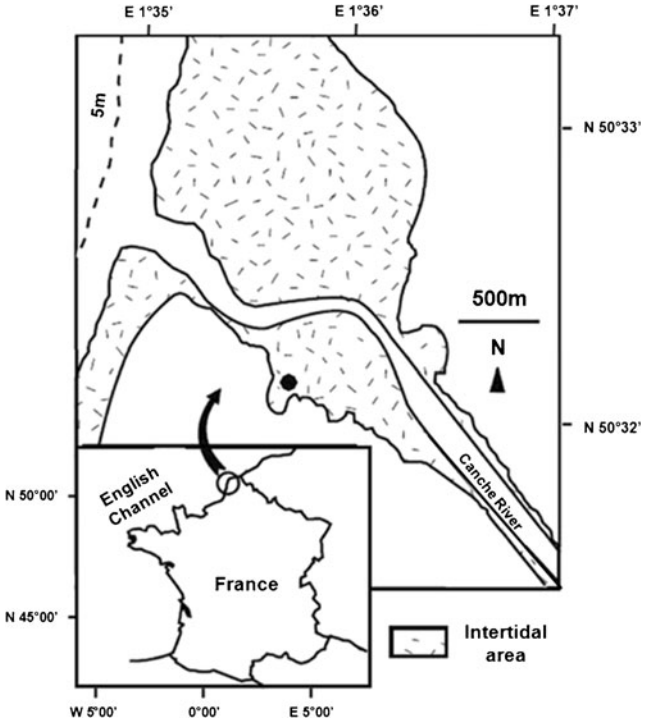

Fig. 1 The Bay of Canche, on the French coast of the eastern English Channel, and the location of the investigated area in the southern mudflat (*black dot*)

covers an area of 630 ha, and the present study was conducted in its southern part (50°32′10″N, 1°35′43″E), in a mudflat sheltered from open-sea waves and strong tidal currents by a slipway. The site is subjected to flooding twice a day (semi-diurnal tide regime) with an average tidal range from ca. 8 m during spring tides to ca. 3 m during neap tides. The deployment was performed during six consecutive days from 22 April to 27 April 2008 with tidal amplitudes decreasing from 7.7 to 4.3 m. The station investigated was located 7.5 m above the lowest low-water level (low-water level of highest astronomical tides).

2.2 Microelectrode measurements

In situ microprofile measurements were performed with an automated portable unit (Miniprofiler MP4; Unisense™) supporting three oxygen microsensors (OX50; Unisense) (described in Denis and Desreumaux (2009)). Clark-type microsensors had an outside tip diameter of 50 μm, a response time <2 s, a stirring sensitivity <2 %, and were calibrated as described by Revsbech (1989).

Before deploying the miniprofiler, three PVC plates were gently positioned to fix the feet of the tripod and prevent lateral movement during measurement. Then, the miniprofiler was deployed carefully, avoiding any disturbance of the study area. Although the miniprofiler might be used autonomously, it was continuously connected to a computer and manually triggered during this deployment, which allowed the visualization of the profiles and the modification of profiling parameters in real time. To avoid changes that could be attributed to the spatial heterogeneity of microphytobenthos, successive profiles were performed at the same location, about every 15–20 min with a vertical resolution of 100 μm, down to a depth of approximately 3–5 mm in the sediment. Profiles were initiated approximately 1 mm above the sediment–water/air interface and down to the anoxic layer, which corresponds to the depth where the microelectrode signal reached zero current (the oxygen penetration depth, O_{pd}). Oxygen partial pressure was converted to oxygen concentration as a function of measured salinity and temperature of surficial sediments (Garcia and Gordon 1992).

Vertical oxygen microprofiles allowed numerical estimations of net oxygen production (NOP) with depth using the Profile numerical model developed by Berg et al. (1998), based on a control volume approach and measured porosity (see below). Vertical integration of production rates allowed the estimation of NOP per unit area. For all calculations, we assumed steady-state and 1D vertical exchange only, while irrigation and bioturbation processes were not considered.

2.3 Physical measurements

Photosynthetically active radiation (PAR) was measured continuously during the 6 days of experimentation using an autonomous plane light sensor (model: ALW-CMP, wavelength: 400–700 nm; Alec Electronics Co. Ltd., Kobe, Japan) equipped with a wiper. This planar sensor was inserted into the sediment close to the miniprofiler and positioned at the level of the sediment–water/air interface. Measurements were performed every 2 s, and an average value was logged every minute.

Temperature of the surficial sediment was measured using a microsensor connected to the miniprofiler (outside tip diameter of 100 μm, 90 % response time of <3 s) which executed the same profiles as the oxygen sensors. This allowed an accurate conversion of oxygen partial pressure values into oxygen concentrations. Values acquired at the end of each profile were used to monitor the temperature evolution during the deployment.

Salinity was checked by sampling sediment cores (inner diameter of 3.5 cm) close to the miniprofiler. Interstitial water was extracted from the first 0.5 cm sediment slice by centrifugation at 3000 rpm for 10 min. A PAL-ES3 (ATAGO™) allowed for the measurement of the salinity in the low volume of sampled water (0.3 ml). Several additional measurements were taken from the water column during immersion periods.

2.4 Sediment characteristics

In order to estimate chlorophyll *a* (Chl *a*) concentrations in the sediment, four cores (inner diameter of 2.6 cm) were randomly sampled close to the miniprofiler at the beginning

and the end of the deployment and stored at −80 °C. Analysis of Chl *a* was undertaken according to the method of Lorenzen (1967) on the upper 1 cm of sediment, where active photosynthetic cells are located (Cadée and Hegeman 1974). Four additional cores (inner diameter of 2.6 cm), sampled close to the study area and stored at −20 °C, were sliced at 0.1 cm intervals down to 1 cm depth and every 0.5 cm down to a depth of 5 cm for the determination of porosity profiles. Porosity was estimated by drying in an oven (80 °C) for 72 h and assuming a dry particle density of 2.65 $g cm^{-3}$ (Mackin and Aller 1984).

2.5 Fluorescence measurements

Concurrent with miniprofiler deployment, modulated fluorescence was measured in situ with a Diving PAM (Heinz Walz, Effeltrich, Germany) under natural irradiance, when meteorological conditions were optimal. PAM measurements were performed in triplicate during the emersion period, every 20 min (time spent by the miniprofiler to measure one series of profiles) when the fluorescent signal was sufficient (the steady-state fluorescence level under ambient light, F_t>130, with higher electronic signal damping and gain (amplification factor) as well as higher intensity of measuring light). The tip of the fluorometer was inserted successively in three supports which were placed on a planar surface of the sediment as described in Migné et al. (2007). The distance to the sediment surface was constant and set to 2 mm. This system allowed for the estimation of the effective quantum yield of the PSII (Φ_{PSII}), according to Genty et al. (1989):

$$\Phi_{PSII} = \frac{(F_m - F_t)}{F'_m} \quad (1)$$

where F_m' is the maximum fluorescence level after a saturating pulse. Acquisition of Φ_{PSII} led to the calculation of the relative electron transport rate (rETR) as follows:

$$rETR = \Phi_{PSII} \times PAR \times 0.5 \quad (2)$$

where PAR (400–700 nm) is in micromole photon per square meter per second; the term relative was used because the specific absorption coefficient was not measured (Underwood 2002; Forster and Kromkamp 2004).

2.6 Data analysis

Photosynthesis versus irradiance curves (*P–I* curves) derived from oxygen measurements were constructed using values of gross oxygen production (GOP) obtained as follows:

$$GOP = NOP - R_e \quad (3)$$

where R_e is the average respiration during emersion (average oxygen consumption measured during dark emersion periods).

P–I curves were then constructed by using values of GOP or rETR measured under the same irradiance at the same time and were fitted to the model of Webb et al. (1974):

$$P = P_m \times \left[1 - \exp\left(\frac{-I}{I_k}\right)\right] \quad (4)$$

where P is GOP (millimole O_2 per square meter per hour) or rETR; P_m is the maximal rate of oxygen production (GOP_m) or maximal rETR ($rETR_m$); I is irradiance (micromole photon per square meter per second), and I_k is the saturation onset parameter. The SPSS Inc. Systat 9© software was used to estimate the photosynthetic parameters (GOP_m or $rETR_m$ and I_k). A photosynthetic quotient of 1 was used to transform GOP values into gross carbon production (Barranguet et al. 1998; Clavier et al. 1994).

3 Results

3.1 Sediment and physical characteristics

The deployment started during the spring tide period and was concluded 6 days later. Maximum tide height varied from 9.13 to 7.79 m on 22 April 2008 and on 27 April 2008, respectively (Fig. 2a), while the tidal amplitude varied from 7.67 to 4.39 m (Table 1). Irradiance values reached up to 2,052 $\mu mol photons\ m^{-2}s^{-1}$ (see Table 1) with, in general, a gradual increase from the sunrise to local noon (see Fig. 2b). In the afternoon, irradiance at the surface of the sediment was affected by the tidal inundation with sharp variations during flooding and ebbing. During the immersion periods, the irradiance signal generally remained lower than 100 $\mu mol photons m^{-2}s^{-1}$. After ebbing, which led to a rapid increase in irradiance level, a gradual decrease was recorded until sunset. During the six consecutive days, only the second day was cloudy and produced low irradiance values (maximum was 771 $\mu mol photons m^{-2}s^{-1}$ recorded at 18:05). The other days showed typical light changes only disrupted by a few cloudy intervals, resulting in sharp drops of light intensity (maximal daily irradiance values ranged from 1,522 to 2,052 $\mu mol m^{-2}s^{-1}$, except on 23 April).

Temperature ranged from 6.9 °C to 19.2 °C between 22 and 27 April (see Fig. 2a) and temperature values generally followed the irradiance curve. Maximal values were recorded at local noon during air exposure, and minimum ones were measured at night. Sediment temperature during nocturnal immersion periods did not show any significant evolution (weekly mean of 11.3±0.3 °C) and was lower than values recorded during diurnal immersion (weekly mean of 12.4±0.9 °C). On the contrary, a decrease of temperature was evidenced during nocturnal emersion periods.

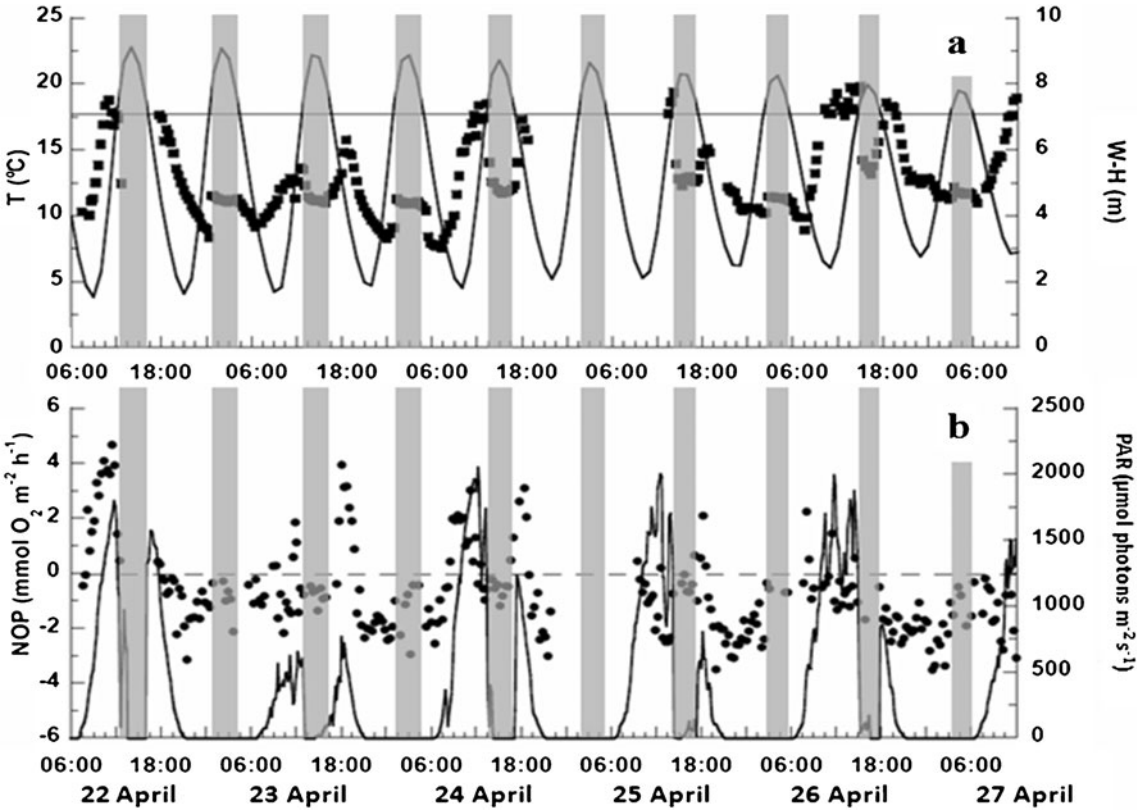

Fig. 2 **a** Temporal variations in surficial sediment temperature (T, *black squares*), water height (W-H, *solid line*) and **b** average net oxygen production (NOP, *black points*), and photosynthetically active irradiance (PAR, *solid line*) at the sediment surface during the whole deployment period (six consecutive days). The *horizontal solid line* on (**a**) represents the altitudinal location of the sediment under investigation and the *gray stripes* represent immersion periods

The biomass of microphytobenthos did not show any significant difference between measurements performed on the first and the last days (Student *t* test, $p=0.37$). High average Chl *a* concentrations were observed in the first centimeter of the sediment (see Table 1).

Average porosity measured during those the first and last days were not statistically different (Kruskal–Wallis test; $n=6$; $P>0.05$). Average porosity values (mean±SD) were close to 1 (0.95±0.01) in the first millimeter, decreased with depth until 1 cm and remained constant beneath the first centimeter with a mean value of 0.90±0.02.

3.2 Calculation of net oxygen production

The microprofiling system monitored oxygen concentrations during all field campaign duration, except the first high tide period (22 April 2008 from 12:20 to 16:40) and the night from 24 to 25 April for technical reasons. A total

Table 1 Environmental characteristics of the study site for each day of the deployment: tidal amplitude, emersion length, chlorophyll *a* concentration in the first centimeter of sediment (Chl *a*, average data ± SD, $n=4$), maximum and mean irradiance

Date	Tidal amplitude (m)	Emersion length (h)	Chl *a* concentration ($mg\,m^{-2}$)	Maximum/mean daily PAR ($\mu mol\ photons\,m^{-2}\,s^{-1}$)
22/04/2008	7.67/7.49	08:34/08:36	240±30	1,796/664
23/04/2008	7.49/7.16	08:38/08:41	–	771/247
24/04/2008	7.13/6.65	08:50/09:05	–	2,052/646
25/04/2008	6.58/5.99	09:08/09:20	–	2,002/615
26/04/2008	5.88/5.21	09:45/10:07	–	1,992/718
27/04/2008	5.05	11:10	259±25	1,522/610

PAR photosynthetically active radiation

number of 932 in situ O_2 microprofiles were thus obtained during the six consecutive days. A few typical profiles and corresponding model fits are shown in Fig. 3. The most representative fits resulted in a number of sediment layers used for Profile model calculations ranging from 3 to 12.

Integrated NOP rates, calculated from oxygen profiles, were established every 20 min throughout the deployment. They ranged from −3.80 to 6.74 mmol$m^{-2}h^{-1}$, with numerous short-term variations (see Fig. 2). Despite the missing data during the diurnal high tide on 22 April, it can be safely assumed that no photosynthesis occurred during immersion. Indeed, values calculated from underwater profiles showed only negative NOP, as light intensity recorded was close to zero. On 22 and 24 April, morning low tides were characterized by the typical light responses of microphytobenthos (Figs. 4a and 5a). After early measurements (before 08:00) which resulted in an average negative NOP, values became positive and sharply increased up to maximal values of 4.66 mmol$m^{-2}h^{-1}$ at 11:28 on 22 April and 3.7 mmolm^{-2} h^{-1} at 11:15 on 24 April. The end of emersion periods was characterized by drops in NOP from 11:47 on 22 April and from 11:35 on 24 April. In the morning of 23 April, NOP remained negative due to low irradiance during this emersion period (maximum of 650 μmol photons $m^{-2}s^{-1}$), except for the three last measurements obtained before flooding. Conversely, in the afternoon, NOP was positive 30 min after ebbing, and a maximum was measured after 50 min, while PAR remained low. On the afternoon of 24 April, ambient light was not disrupted by clouds and the time lag between ebbing and positive NOP was 20 min, while maximal values were observed 40 min after ebbing. The last 3 days did not show the same pattern. While temperature and irradiance showed similar values to those measured during the first days, very few calculated NOP values were positive.

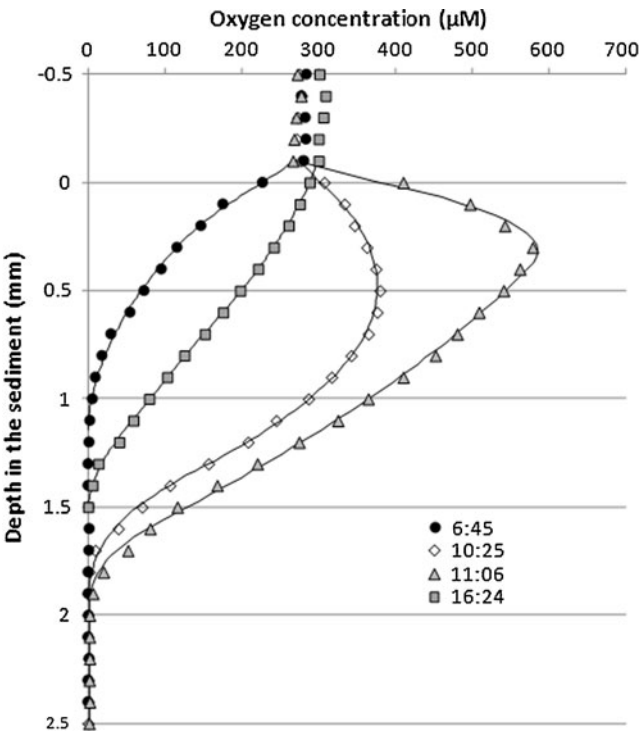

Fig. 3 Typical oxygen profiles obtained on 24 April at 6:45 (emersion, dark—*black circles*), at 10:25 (emersion, low irradiance—*open diamonds*), at 11:06 (emersion, high irradiance—*gray triangles*) and at 16:24 (immersion, dark—*gray squares*). *Symbols* correspond to oxygen concentrations measured with the first sensor, and lines are the corresponding fits obtained with the Profile model (Berg et al. 1998)

Oxygen penetration depth (O_{pd}, ±SD) ranged from 0.5 to 4.5 mm with a mean value of 1.6±0.7 mm. During daily emersion, O_{pd} ranged from 0.7 to 4.5 mm (mean value 1.6± 0.5 mm) and was close to O_{pd} measured at immersion (in the range 0.8–3.3 mm; mean value 1.7±0.5), whereas it was statistically different ($P<0.001$) during nocturnal emersions, O_{pd} values ranging from 0.5 to 1.4 mm (mean value 1.1±0.3 mm).

3.3 Fluorescence measurements

Simultaneous measurements of Φ_{PSII} were performed during the mornings of 22 and 24 April 2008, and consequently, rETR were calculated (see Figs. 4b and 5b). Triplicate oxygen profiles and triplicate measurements of fluorescence parameters were thus acquired simultaneously between 07:20 and 12:10 on 22 April (see Fig. 4b) and between 06:20 and 12:30 on 24 April (see Fig. 5b).

Values of rETR acquired on 22 April showed a rapid increase from 07:30 (22±0.16) to 10:50 (97±9.0) and decreased later on before flooding, with a value of 76±11 measured 50 min before immersion. On 24 April, the evolution of rETR between 07:30 and 09:30 was very similar, but from 09:30 to 12:30, rETR remained stable (90±7.8; $n=18$) until flooding.

3.4 Photosynthesis–irradiance curves

For both days, the range of irradiance was sufficiently large and the photosynthesis response was clearly marked so that *P–I* curves were established using GOP and rETR values. All oxygen consumption measurements in the dark and during emersion were averaged for each day, and values obtained for R_e (1.8±0.4 mmol$m^{-2}h^{-1}$ on 22 April and 2.1±0.6 mmolm^{-2} h^{-1} on 24 April) were used to calculate GOP values (while R_e ranged from 0.4 to 3.5 mmol$m^{-2}h^{-1}$ during the whole deployment). GOP and rETR values plotted as a function of irradiance as well as fitted *P–I* curves derived from those results are given (Fig. 6). For GOP, encircled data correspond to values acquired just before flooding (after 11:30 on 22 April and after 11:15 on 24 April) and were not included in the calculations of *P–I* curves (see "Discussion" section for details). Models (Table 2) explained more than 80 % of the variability for each *P–I* curve.

No clear change in maximum rates of photosynthesis (GOP_m or $rETR_m$) was observed between 22 and 24 April

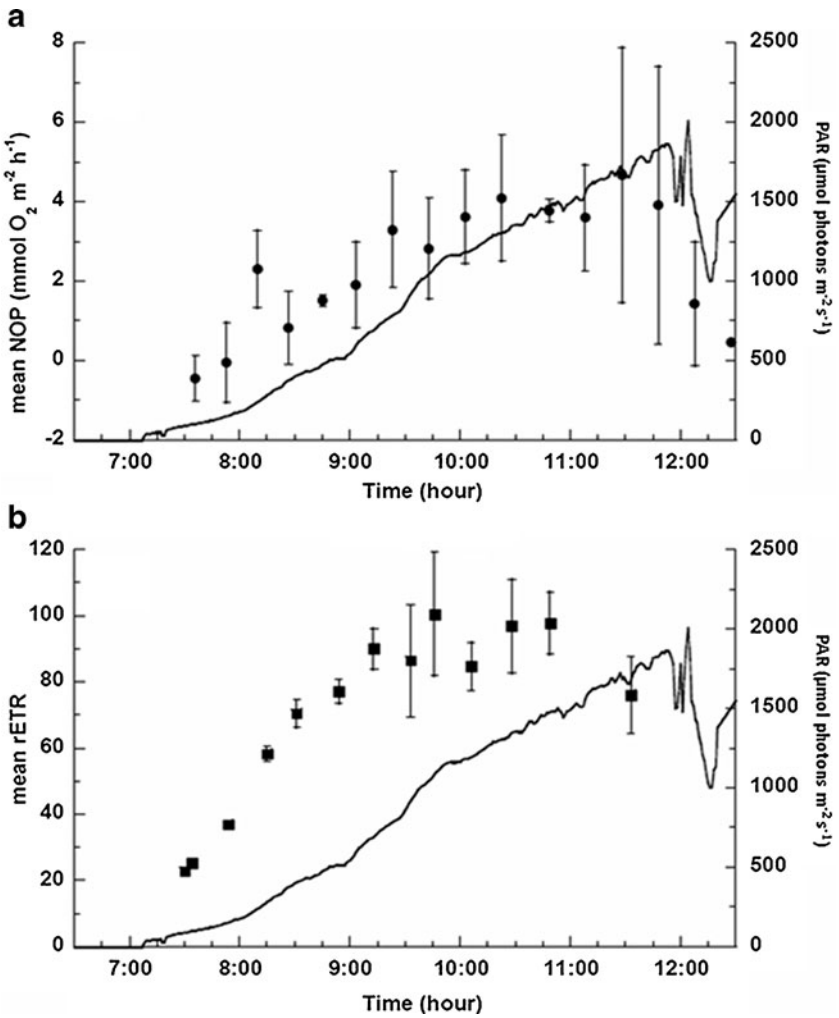

Fig. 4 Temporal variation in **a** mean net oxygen production (mean NOP, ±SD, n=3, *black points*), **b** mean relative electron transport rate (mean rETR, ±SD, n=3, *black squares*) and photosynthetically active irradiance (PAR, *solid lines*) measured during low tide on 22 April 2008

(see Table 2), while the saturation onset parameter (I_k) showed marked differences. Indeed, on 22 April, I_k derived from rETR data was 1.6 times lower than I_k calculated from GOP.

Parallel measurements allowed the establishment of a relationship between gross carbon production (GCP, obtained after conversion of GOP values into carbon values) and rETR (Fig. 7). A linear correlation between mean rETR and GCP was obtained on 22 April (n=12; r=0.81; P<0.01) as well as on 24 April with a higher significance (n=15; r=0.94; P< 0.001). Both relationships were in strong accordance and, when compiling values acquired during both days, the correlation was also highly significant (n=27; r=0.90; P<0.001).

4 Discussion

4.1 Relation between microphytobenthic production and light intensity

In the present study, the maximum NOP value measured during the deployment (4.3 mmolO_2 $m^{-2}h^{-1}$, when considering average values from triplicate profiles) was generally in line with other studies using microsensors in intertidal areas. For instance, Epping and Jorgensen (1996) obtained NOP values up to 4.9 mmol$O_2m^{-2}h^{-1}$ for intertidal sediments located near Texel (The Netherlands), while Gerbersdorf et al. (2005) reported NOP up to 5 mmol$O_2m^{-2}h^{-1}$ in the estuarine Bodden area of the southern Baltic Sea (Germany). In contrast, using the same equipment as the present study, Denis and Desreumaux (2009) reported maximal NOP of 9.4 mmol$O_2m^{-2}h^{-1}$ for the same site and season (13 April 2007) and similar PAR intensities, despite lower chlorophyll *a* content. These authors also recorded large variations, as they reported maximal NOP around 1.4 mmol$O_2m^{-2}h^{-1}$ 1 week later, the change being attributed to the accumulation of polychaete tubes at the surface of the sediment, acting as a filter drastically decreasing the available light for microphytobenthos.

During the survey, three different periods regarding the daily relation between oxygen production and light intensity could be identified:

- 22 and 24 April: during the first emersion period of these 2 days, we observed a typical response of NOP

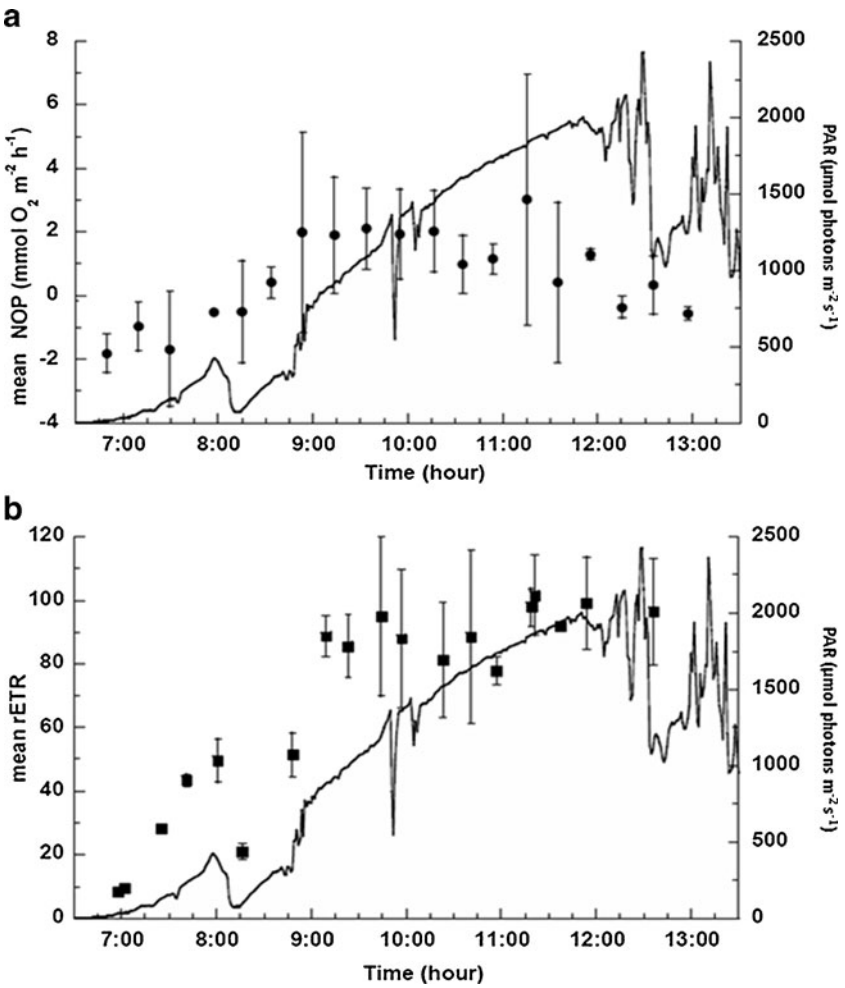

Fig. 5 Temporal variation in **a** mean net oxygen production (mean NOP, ±SD, n=3, *black points*), **b** mean relative electron transport rate (mean rETR, ±SD, n=3, *black squares*) and photosynthetically active irradiance (PAR, *solid lines*) measured during low tide on 24 April 2008

to light intensity whereas lower NOP were recorded in the afternoon despite high irradiance values (>1,000 µmol photons $m^{-2}s^{-1}$);

- 23 April: low irradiance values were recorded throughout the day (<750 µmol photons $m^{-2}s^{-1}$) and concomitantly NOP remained close to zero in the morning. After flooding, measurements showed higher NOP during emersion (up to 3.93±1.72 mmol O_2 $m^{-2}h^{-1}$) and a good relationship between NOP and light intensity (R^2=0.92); and
- 25 to 27 April: the last 3 days showed high irradiance values while NOP rate remained low (generally negative), and consequently, there were poor relationships between NOP and light intensity.

The consideration of the short-term variability of microphytobenthic primary production is essential in order to produce realistic primary production estimations (MacIntyre and Cullen 1996). However, the high-frequency variation in microphytobenthic primary production remains difficult to follow and is consequently scarcely documented. The microphytobenthic production, as measured during the present survey, demonstrated large temporal changes in efficiency as well as in intensity. The causes of the decrease in primary production as observed during this in situ study are hardly identifiable owing to superimposition of numerous environmental and biological factors. However, low NOP rates measured on 22 and 24 April during the second emersion periods of day might have been due to a resuspension event, known to cause a sharp reduction of microphytobenthic production (Peletier 1996; Kingston 1999; Montani et al. 2003). Low NOP rates could also be due to high irradiance exposure encountered in the morning. This might cause strong photo-inhibition which could not be recovered during dark immersion periods. However, photo-inhibition is generally not observed in microphytobenthic communities (Rasmussen et al. 1983; Barranguet et al. 1998; Chevalier et al. 2010) because downward migration (Pinkney and Zingmark 1991; Consalvey et al. 2004) as well as migratory micro-cycles (Kromkamp et al. 1998; Kingston 1999) prevent the exposure of cells to high incident light.

On 23 April, NOP measured during the afternoon was comparable to those measured on 22 and 24 April in the morning, while irradiance did not exceed 750 µmol photons $m^{-2}s^{-1}$. Serôdio et al. (2008) previously observed that photosynthetic activity was drastically affected by irradiance

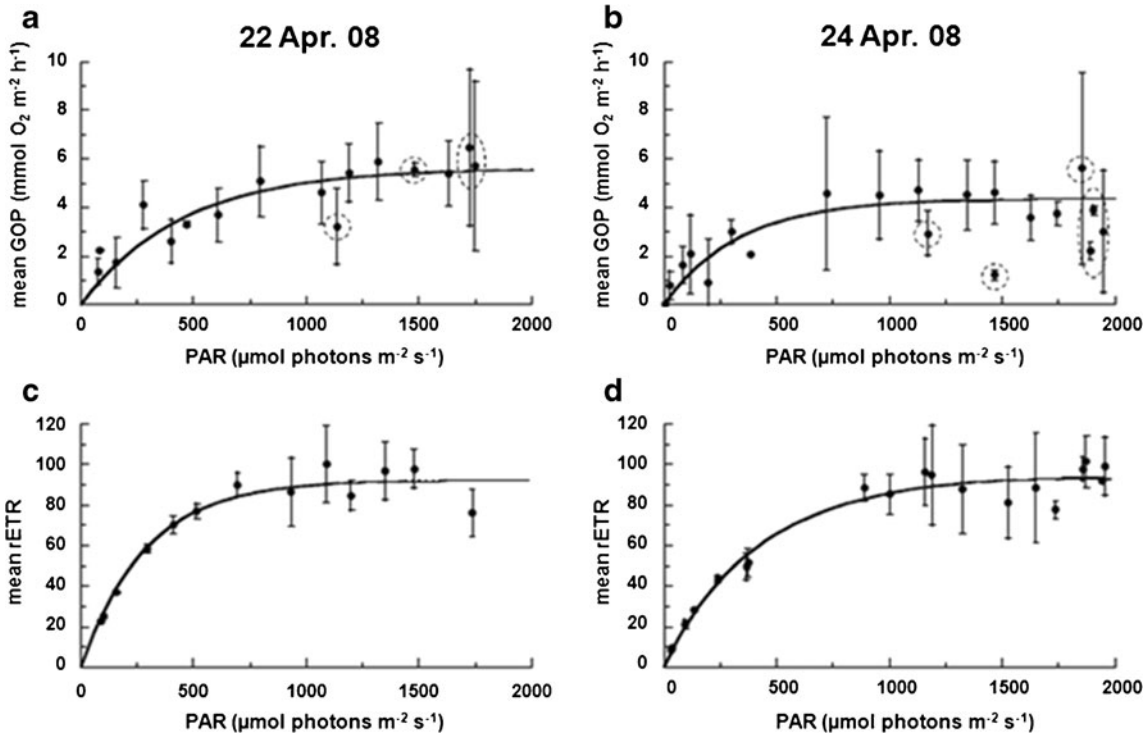

Fig. 6 Average gross oxygen production (GOP, **a** and **b**) and relative electron transport rate (rETR, **c** and **d**) measured simultaneously under varying photosynthetically active irradiance (PAR) on 22 April 2008 and 24 April 2008. *Solid lines* are composite photosynthesis–irradiance (*P–I*) curves obtained using the model of Webb et al. (1974); for parameters, see Table 2. *Encircled data* were not used on *P–I* curves calculations (see text for details)

received during morning emersion periods, which may explain these values, as light intensity was very low on the morning.

Other emersion periods were marked by a low negative NOP, while irradiance was high. Negative NOP observed at the end of the field campaign (from 25 to 27 April) under normal irradiance suggested an important perturbation of the benthic primary production, which might be due to the repetitive insertion of the sensors into the exact same place during the whole monitoring period. Indeed, of approximately 65 triplicate oxygen profiles performed during diurnal emersion periods, only nine resulted in positive NOP. The huge difference observed between the first 3 days and the end of the campaign cannot be clearly related to resuspension events, as Chl *a* concentrations did not show any significant change between the beginning and the end of the survey (240±30 and 259±25 mgChl $a\,m^{-2}$ on 22 and 27 April, respectively). Low temperature variations during emersion periods excluded this factor as a possibility to explain the drastic change observed here. Numerous other physical, chemical and/or biological factors, such as sediment resuspension (de Jonge and Van Beusekom 1992), nutrient limitation (Kingston 2002), or macrofaunal grazing (Cahoon 1999; Blanchard et al. 2000), may explain a sharp decrease of primary production. The time-lag between flooding time at the beginning and the end of the survey

Table 2 Parameters derived from fitted photosynthesis–irradiance (*P–I*) curves based on the model of Webb (see text for details)

Date	Fluorescence measurements				Oxygen microprofiles			
	$rETR_m$	I_k	*n*	R^2	GOP_m	I_k	*n*	R^2
22/04/2008	92.5	287	13	0.94	5.7	427	12	0.90
24/04/2008	93.0	387	19	0.93	4.4	315	14	0.89

Maximum rates of relative electron transport rate ($rETR_m$, arbitrary unit, for fluorescence measurements) or gross oxygen production (GOP_m, mmol $m^{-2}\,h^{-1}$, for microprofiles measurements), saturation onset parameter (I_k, µmol photons $m^{-2}\,s^{-1}$), data number used in the calculations (*n*) and the determination coefficient R^2 corresponds to the goodness-of-fit between measured and simulated primary production for measurements performed during morning emersion periods on 22 and 24 April 2008

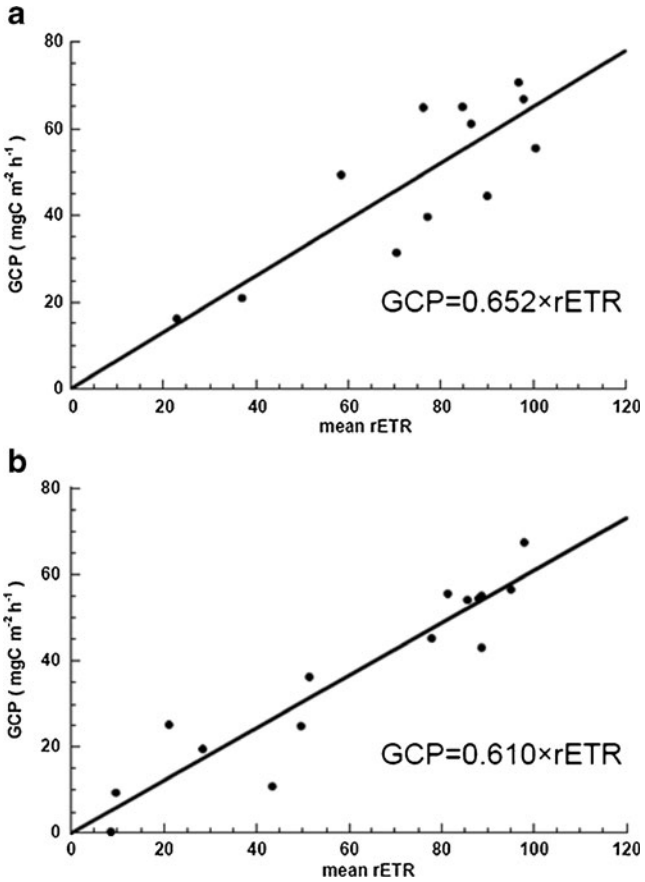

Fig. 7 Relationship between mean relative electron transport rate (mean rETR) and average gross carbon production (GCP) derived from gross oxygen production (GOP) based on data obtained on **a** 22 April (n=12; r=0.81; P<0.01) and **b** 24 April (n=15; r=0.94; P<0.001)

(and consequent higher duration of the emersion period, causing enhanced desiccation), as well as the previous "history" of microphytobenthic communities before the deployment, might also play a significant role in the evolution observed. Moreover, a drastic reduction of primary production has already been observed in the same area due to a pulse input of tubes and juveniles of the polychaete species *Lanice conchilega* drastically decreasing the light availability at the surface of the sediments and hence photosynthetic activity (Denis and Desreumaux 2009). All factors potentially involved were not clearly identified and no robust hypothesis can be proposed.

However, our study has shown the necessity of microphytobenthic primary production surveys at high frequency in order to calculate more consistent and accurate temporal budgets. For instance, calculations using in situ continuous measurements of oxygen profiles during the whole study led to a GOP of 165 $mmolO_2m^{-2}$ for the whole survey (128 h long, from 22 April 6:00 to 27 April 12:00) or an average GOP of 1.29 $mmolO_2m^{-2}h^{-1}$. Conversely, P–I curve parameters acquired on 22 April (see Fig. 6a; Table 2) and irradiance values recorded during the whole survey led to an estimated GOP of 238 $mmolO_2m^{-2}$ for the same period (1.86 $mmolO_2m^{-2}h^{-1}$), i.e., an overestimation of 31 %. Spilmont et al. (2007) and Migné et al. (2009) previously highlighted the relevance of the inclusion of the short-term variability in annual budget calculations, with an overestimation of ca. 40–50 % when such variability was not taken into account. Moreover, as stressed by the previous authors, it is critical to develop production models that consider the variability of the processes at several time scales, ranging from hourly to seasonal, particularly when results are extrapolated. The monitoring of oxygen fluxes using microelectrodes thus appears useful to reveal the short-term variability which might be difficult to detect with "classical" methods (e.g., benthic chambers), hence the relevance of the combined use of these different methods for the calculation of annual budgets.

4.2 Migration behavior

Even if the large changes recorded at the end of the deployment remain unexplained, the first 3 days were marked by sharp decreases of NOP before flooding, reaching values close to zero or negative. These important drops before flooding may be related to the migration behavior of the epipelic community, which largely dominates intertidal mudflats. Moreover, the high standard deviations calculated from oxygen profiles acquired at the end of the emersion period might be due to non-synchronous migration behavior which led to large differences between the three profiles performed at the same time.

The time lag between NOP_{max} and flooding varied between 60 and 120 min. Previous estimations of this time lag performed on an intertidal mudflat located in the English Channel (Bay of Somme) showed a primary production which decreased approximately 100 min before flooding (Spilmont et al. 2007). On 23 April, despite low irradiance, an important decrease of NOP occurred 70 min before flooding, which suggested an endogenous rhythm, surpassing the necessary access to light of microphytobenthic organisms. On 24 April, sharp variations in PAR due to clouds observed before flooding led to low NOP values, hence interfering with the expected measurement of migratory behavior. Migratory behavior is well known in microphytobenthic communities living in muddy sediments of intertidal areas (see Consalvey et al. 2004), as well as in subtidal areas (Ni Longphuirt et al. 2007), and is considered as an evolutionary survival advantage for these organisms (Kingston 1999). Different scenarios occurring before flooding have been suggested by Consalvey (2002). The microphytobenthic compartment can show high Chl *a* concentration in surficial sediments during immersion, but their association with high Extracellular Polymeric Substances (EPS) concentrations may avoid resuspension events

(Easley et al. 2005). However, in intertidal mudflats, downward migration has generally been described (Paterson 1986; Serôdio et al. 1997; Barranguet et al. 1998; Honeywill 2001, Honeywill et al. 2002). Herlory et al. (2004) observed an asymmetric pattern with, on the one hand rapid upward movements at the beginning of emersion, and on the other hand a slower downward migration before flooding. NOP values measured during afternoon emersion did not show any clear response, but on 23 April, the low irradiance recorded during the morning led to microphytobenthos responding by optimizing photosynthetic activity in the afternoon, even while PAR remained low.

4.3 Gross carbon production and relationships between fluorescence and oxygen methods

The integrated spatial area is very much smaller for microsensors than for benthic chambers or ^{14}C based techniques (MacIntyre and Cullen 1996). Consequently, due to the spatial heterogeneity of microphytobenthos (Spilmont et al. 2011), the use of oxygen microelectrodes is generally restricted to the descriptive processes approach, rather than carbon production estimates. However, by using three sensors, we partly took into account the small-scale spatial variability and estimations of primary production should be more realistic. Since the microprofiler was not moved between measurements, the observed variations were due only to temporal changes in the activity of microorganisms in response to chemical and physical factors and not to spatial heterogeneity. Moreover, the objective here was to compare the short-term variability to the seasonal variability and not to extrapolate production budgets. The m^2 scale was used as a reference unit for convenience and for comparison with published data. Still, it is clear that GCP estimates acquired punctually may not be as representative as the ones obtained from other methods based on larger areas (Spilmont et al. 2011). However, microelectrodes are, to date, the only tool that allows the continuous high-frequency monitoring of in situ oxygen fluxes, over large time periods (6 days in the present study), and during emersion, emersion, and the transition periods. The estimated GCP in the present study varied between 3 and 90 $mgCm^{-2}h^{-1}$. Previous measurements performed with benthic chambers or ^{14}C uptake in different intertidal muddy sediment in the English Channel showed values in the same range: from 3 to 150 $mgCm^{-2}h^{-1}$ in the Somme bay (Migné et al. 2004), from 0 to 122 $mgCm^{-2}h^{-1}$ in the Seine estuary (Spilmont et al. 2006), and from 5 to 100 $mgCm^{-2}h^{-1}$ in the Westerschelde (SW Netherlands) (Barranguet et al. 1998).

The strong relationships between GCP (assessed here by oxygen microprofiling system) and rETR have also been pointed out by Migné et al. (2007) and Davoult et al. (2009) with benthic chambers. By pooling the data obtained on 22 and 24 April, the relationship gave a conversion rate from rETR to GCP expressed in carbon units (slope=0.630, n=27, r=0.90) close to the one highlighted by Migné et al. (2007; slope=0.744, n=106, r=0.93), who gathered data from different sites (the bay of Somme, the Seine estuary and the bay of Authie). Thus, a conversion coefficient between GCP and rETR of about 0.7 seems to be a general rule, but measurements in other systems as well as the verification of photosynthetic quotient should be prerequisites before widely applying such a coefficient.

5 Conclusions

The use of an automated system allowed the estimation of sediment–water or sediment–air oxygen exchanges at high frequency (every 20 min) during both immersion and emersion periods. No methodological change or adaptation was needed to acquire data, whereas in situ high-frequency measurements of CO_2 exchange rates or fluorescence measurements during both emersion and immersion are difficult. To our knowledge, this is the first study presenting continuous measurements of sediment–water/air exchanges during six consecutive days in an intertidal area. A high short-term variability was shown, with drastic modifications of oxygen production, mainly linked to the migratory behavior of microphytobenthic organisms, and perhaps to resuspension events. We have shown the downward migration of epipelic microphytobenthos in situ before flooding. We are aware that the small spatial area covered by microelectrodes is a limitation in providing realistic spatial estimations, even if several sensors are used simultaneously, but as short-term temporal variability seems to be widely affected by several environmental factors, the possibility of recording such "key events" and being able to integrate them in temporal budgets may counterbalance their poor spatial coverage. These results suggest that an automated microprofiling system for future calculations of microphytobenthic production is useful and versatile since the equipment might also be used in sandy sediments, where hydrodynamic influence and interstitial water renewal make the use of other designs problematic.

Acknowledgments The authors would like to acknowledge the University Lille 1 which, through BQR funding, supported this project. We are also indebted to several students who took part in this project, especially Pierre-Emmanuel Desreumaux who performed a large part of the field measurements. Moreover, the authors are grateful to two anonymous reviewers for their detailed comments, which contributed greatly to improving the quality of the manuscript.

References

Barranguet C, Kromkamp J (2000) Estimating primary production rates from photosynthetic electron transport in estuarine microphytobenthos. Mar Ecol Prog Ser 204:39–52

Barranguet C, Kromkamp J, Peene J (1998) Factors controlling primary production and photosynthetic characteristics of intertidal microphytobenthos. Mar Ecol Prog Ser 173:117–126

Berg P, Risgaard-Petersen N, Rysgaard S (1998) Interpretation of measured concentration profiles in sediment pore water. Limnol Oceanogr 43:1500–1510

Blanchard GF, Paterson DM, Stal LJ, Richard P, Galois R, Huet V, Kelly JA, Honeywill C, De Brouwer JFC, Dyer K, Christie M, Seguignes M (2000) The effect of geomorphological structures on potential biostabilisation by microphytobenthos on intertidal mudflats. Cont Shelf Res 20:1243–1256

Blanchard GF, Agion T, Guarini JM, Herlory O, Richard P (2006) Analysis of the short-term dynamics of microphytobenthos biomass on intertidal mudflats. In: Kromkamp JC, de Brouwer J, Blanchard GF, Forster RM, Créach V (eds) Functioning of microphytobenthos in estuaries. The Academy of Arts and Sciences/The University of Chicago Press, Amsterdam/Chicago, pp 85–98

Cadée GC, Hegeman J (1974) Primary production of the benthic microflora living on tidal flats in the Dutch Wadden Sea. Netherlands. J Sea Res 8:260–291

Cahoon LB (1999) The role of benthic microalgae in neritic ecosystems. Oceanogr Mar Biol Ann Rev 37:47–86

Carrère V, Spilmont N, Davoult D (2004) Comparison of simple techniques for estimating chlorophyll a concentration in the intertidal zone using high spectral-resolution field-spectrometer data. Mar Ecol Prog Ser 274:31–40

Chevalier EM, Gevaert F, Créach A (2010) In situ photosynthetic activity and xanthophylls cycle development of undisturbed microphytobenthos in an intertidal mudflat. J Exp Mar Biol Ecol 385:44–49

Clavier J, Boucher G, Garrigue C (1994) Benthic respiratory and photosynthetic quotients in a tropical lagoon CR. Acad Sci Paris 10:937–942

Cloern JE (1987) Turbidity as a control on phytoplankton biomass and productivity in estuaries. Cont Shelf Res 7:1367–1381

Consalvey M (2002) The structure and function of microphytobenthic biofilms. PhD dissertation, University of St. Andrews, Scotland

Consalvey M, Paterson DM, Underwood GJC (2004) The ups and downs of life in benthic biofilms: migration of benthic diatoms. Diatom Res 19:181–202

Davoult D, Migné A, Créach A, Gevaert F, Hubas C, Spilmont N, Boucher G (2009) Spatio-temporal variability of intertidal benthic primary production and respiration in the western part of the Mont Saint-Michel Bay (Western English Channel, France). Hydrobiologia 620:163–172

De Jonge VN, Van Beusekom JEE (1992) Contribution of resuspended microphytobenthos biomass to total phytoplankton in the Ems estuary and its possible role for grazers. Neth J Sea Res 30:91–105

Denis L, Desreumaux PE (2009) Short-term variability of intertidal microphytobenthic production using an oxygen microprofiling system. Mar Fresh Res 60:712–726

Easley JT, Hymel SN, Plante CJ (2005) Temporal patterns of benthic microalgae migration on a semi-protected beach. Estuar Coast Shelf Sci 64:486–496

Epping EHG, Jørgensen BB (1996) Light-enhanced oxygen respiration in benthic phototrophic communities. Mar Ecol Prog Ser 139:193–203

Forster RM, Kromkamp JC (2004) Modelling the effects of chlorophyll fluorescence from subsurface layers on photosynthetic efficiency measurements in microphytobenthic algae. Mar Ecol Prog Ser 284:9–22

Garcia HE, Gordon LI (1992) Oxygen solubility in seawater. Better fitting equations. Limnol Oceanogr 37:1307–1312

Genty B, Briantais JM, Baker NR (1989) The relationship between the quantum yield of photosynthetic electron transport and quenching of chlorophyll fluorescence. Biochim Biophy Acta 990:87–92

Gerbersdorf SU, Meyercordt J, Meyer-Reil LA (2004) Microphytobenthic primary production within the flocculent layer, its fractions and aggregates, studied in two shallow Baltic estuaries of different eutrophic status. J Exp Mar Biol Ecol 307:47–72

Gerbersdorf SU, Meyercordt J, Meyer-Reil LA (2005) Microphytobenthic primary production in the Bodden estuaries, southern Baltic Sea, at two study sites differing in trophic status. Mar Ecol Prog Ser 41:181–198

Glud RN, Ramsing NB, Revsbech NP (1992) Photosynthesis and photosynthesis coupled respiration in natural biofilms quantified with oxygen microelectrodes. J Phycol 28:51–60

Glud RN, Gundersen JK, Revsbech NP, Jørgensen BB (1994) Effects on the benthic diffusive boundary layer imposed by microelectrodes. Limnol Oceanogr 39:462–467

Glud RN, Ramsing NB, Gundersen JK, Klimant I (1996) Planar optrodes, a new tool for fine scale measurements of two-dimensional O2 distribution in benthic communities. Mar Ecol Prog Ser 140:217–226

Glud RN, Kühl M, Kohls O, Ramsing NB (1999) Heterogeneity of oxygen production and consumption in a photosynthetic microbial mat as studied by planar optodes. J Phycol 35:270–279

Glud NR, Kühl M, Wenzhöfer F, Rysgaard S (2002) Benthic diatoms of a high Arctic Fjord (Young Sound, NE Greenland): importance for ecosystem primary production. Mar Ecol Prog Ser 238:15–29

Guarini JM, Blanchard GF, Bacher C, Gros P, Riera P, Richard P, Gouleau D, Galois R, Prou J, Sauriau PG (1998) Dynamics of spatial patterns of microphytobenthic biomass: inferences from a geostatistical analysis of two comprehensive surveys in Marennes-Oléron Bay (France). Mar Ecol Prog Ser 166:131–141

Herlory O, Guarini JM, Richard P, Blanchard GF (2004) Microstructure of microphytobenthic biofilm and its spatio-temporal dynamics in an intertidal mudflat (Aiguillon Bay, France). Mar Ecol Prog Ser 282:33–44

Honeywill C (2001) In situ analysis of the biomass and distribution of microphytobenthos. PhD dissertation, University of St. Andrews, Scotland

Honeywill C, Paterson DM, Hagerthey SE (2002) Determination of microphytobenthic biomass using pulse-amplitude modulated minimum fluorescence. Br Phycol J 37:485–492

Jørgensen BB, Boudreau BP (2001) Diagenesis and sediment—water exchange. In: Boudreau BP, Jørgensen BB (eds) The benthic boundary layer: transport processes and biogeochemistry. Oxford University Press, UK, pp 211–244

Kingston MB (1999) Effect of light on vertical migration and photosynthesis of Euglena proxima (Euglenophyta). J Phycol 35:245–253

Kingston MB (2002) Effect of subsurface nutrient supplies on the vertical migration of *Euglena proxima* (Euglenophyta). J Phycol 38:872–880

Kromkamp JC, Forster RM (2006) Developments in microphytobenthos primary productivity studies. In: Kromkamp JC, de Brouwer J, Blanchard GF, Forster RM, Créach V (eds) Functioning of microphytobenthos in estuaries. The Academy of Arts and Sciences/The University of Chicago Press, Amsterdam/Chicago, pp 165–183

Kromkamp JC, Barranguet C, Peen J (1998) Determination of microphytobenthos PSII quantum efficiency and photosynthetic activity by means of variable chlorophyll fluorescence. Mar Ecol Prog Ser 162:45–55

Lorenzen CJ (1967) Determination of chlorophyll and phaeopigments: spectrophotometric equations. Limnol Oceanogr 12:343–346

MacIntyre HL, Cullen JJ (1996) Primary production by suspended and benthic microalgae in a turbid estuary: time-scales of variability in San Antonio Bay, Texas. Mar Ecol Prog Ser 145:245–268

Mackin JE, Aller JC (1984) Ammonium adsorption in marine sediments. Limnol Oceanogr 29:250–257

Migné A, Davoult D, Spilmont N, Menu G, Boucher G, Gattuso JP, Rybarczyk H (2004) In situ measurements of benthic primary production during emersion: seasonal variations and annual production in the Bay of Somme (Eastern English Channel, France). Cont Shelf Res 24:1437–1449

Migné A, Gevaert F, Creach A, Spilmont N, Chevalier E, Davoult D (2007) Photosynthetic activity of intertidal microphytobenthic communities during emersion: in situ measurements of chlorophyll fluorescence (PAM) and CO2 flux (IRGA). J Phycol 43:864–873

Migné A, Spilmont N, Boucher G, Denis L, Hubas C, Janquin M-A, Rauch M, Davoult D (2009) Annual budget of benthic production in Mont Saint Michel Bay considering cloudiness, microphytobenthos migration, and variability of respiration rates with tidal conditions. Cont Shelf Res 29:2280–2285

Montani S, Magni P, Abe N (2003) Seasonal and interannual patterns of intertidal microphytobenthos in combination with laboratory and areal production estimates. Mar Ecol Prog Ser 249:79–91

Ni Longphuirt S, Clavier J, Grall J, Chauvaud L, Le Loc'h F, Le Berre I, Flye-Sainte-Marie J, Richard J, Leynaert A (2007) Primary production and spatial distribution of subtidal microphytobenthos in a temperate coastal system, the Bay of Brest, France. Estuar Coast Shelf Sci 74:367–380

Paterson DM (1986) The migratory behaviour of diatom assemblages in a laboratory tidal micro-ecosystem examined by low temperature scanning electron microscopy. Diatom Res 1:227–239

Paterson DM, Wiltshire KH, Miles A, Blackburn J, Davidson I, Yates MG, McGrorty S, Eastwood JA (1998) Microbiological mediation of spectral reflectance from intertidal cohesive sediments. Limnol Oceanogr 43:1207–1221

Peletier H (1996) Long-term changes in intertidal estuarine diatom assemblages related to reduced input of organic waste. Mar Ecol Prog Ser 137:265–271

Perkins RG, Oxborough K, Hanlon ARM, Underwood GJC, Baker NR (2002) Can chlorophyll fluorescence be used to estimate the rate of photosynthetic electron transport within microphytobenthic biofilms? Mar Ecol Prog Ser 228:47–56

Pinckney J, Zingmark RG (1991) Effect of tidal stage and sun angles on intertidal benthic microalgal productivity. Mar Ecol Prog Ser 76:81–89

Pinckney J, Zingmark RG (1993) Biomass and production of benthic microalgal communities in five typical estuarine habitats. Estuaries 16:881–891

Rasmussen MB, Henriksen K, Jensen A (1983) Possible causes of temporal fluctuations in primary production of the microphytobenthos in the Danish Wadden Sea. Mar Biol 73:109–114

Revsbech NP (1989) An oxygen microelectrode with a guard cathode. Limnol Oceanogr 34:472–476

Revsbech NP, Jørgensen BB (1983) Photosynthesis of benthic microflora measured with high spatial resolution by the oxygen microprofile method: capabilities and limitations of the method. Limnol Oceanogr 28:749–756

Revsbech NP, Jørgensen BB, Brix O (1981) Primary production of microalgae in sediments measured by oxygen microprofile, $H^{14}CO_3^-$ fixation, and oxygen exchange methods. Limnol Oceanogr 26:717–730

Serôdio J, Marque da Silva J, Catarino F (1997) Non destructive tracing of migratory rhythms of intertidal benthic microalgae using in vivo chlorophyll a fluorescence. J Phycol 33:542–553

Serôdio J, Vieira S, Cruz S, Barroso F (2005) Short-term variability in the photosynthetic activity of microphytobenthos as detected by measuring rapid light curves using variable fluorescence. Mar Biol 146:903–914

Serôdio J, Vieira S, Barroso F (2007) Relationship of variable chlorophyll fluorescence indices to photosynthetic rates in microphytobenthos. Aquat Microb Ecol 49:71–85

Serôdio J, Vieira S, Cruz S (2008) Photosynthetic activity, photoprotection and photoinhibition in intertidal microphytobenthos as studied in situ using variable chlorophyll fluorescence. Cont Shelf Res 28:1363–1375

Spilmont N, Davoult D, Migné A (2006) Benthic primary production during emersion: in situ measurements and potential primary production in the Seine Estuary (English Channel, France). Mar Poll Bull 53:49–55

Spilmont N, Migné A, Seuront L, Davoult D (2007) Short term variability of intertidal benthic community production during emersion and implication in annual budget calculation. Mar Ecol Prog Ser 333:95–101

Spilmont N, Seuront L, Meziane T, Welsh DT (2011) There's more to the picture than meets the eye: sampling microphytobenthos in a heterogeneous environment. Estuar Coast Shelf Sci 95:470–476

Underwood GJC (2002) Adaptations of tropical marine microphytobenthic assemblages along a gradient of light and nutrient availability in Suva Lagoon, Fiji. Eur J Phycol 37:449–462

Webb WL, Newton M, Starr D (1974) Carbon dioxide exchange of *Almus rubra*: a mathematical model. Oecologia 17:281–291

Wenzhöfer F, Glud RN (2004) Small-scale spatial and temporal variability in coastal benthic O2 dynamics: effects of faunal activity. Limnol Oceanogr 49:1471–1481